Research Article Vol. 10, No. 11 / November 2023 / Optica 1543

Thermal intermodulation backaction in a high-cooperativity optomechanical system

Christian M. Pluchar, Aman R. Agrawal, and Dalziel J. Wilson*

Wyant College of Optical Sciences, University of Arizona, Tucson, Arizona 85721, USA
**dalziel.wilson@gmail.com*

Received 18 July 2023; revised 26 September 2023; accepted 12 October 2023; published 15 November 2023

The pursuit of room temperature quantum optomechanics with tethered nanomechanical resonators faces stringent challenges owing to extraneous mechanical degrees of freedom. An important example is thermal intermodulation noise (TIN), a form of excess optical noise produced by mixing of thermal noise peaks. While TIN can be decoupled from the phase of the optical field, it remains indirectly coupled via radiation pressure, implying a hidden source of backaction that might overwhelm shot noise. Here we report observation of TIN backaction in a high-cooperativity, room temperature cavity optomechanical system consisting of an acoustic-frequency Si_3N_4 trampoline coupled to a Fabry–Perot cavity. The backaction we observe exceeds thermal noise by 20 dB and radiation pressure shot noise by 40 dB, despite the thermal motion being 10 times smaller than the cavity linewidth. Our results suggest that mitigating TIN may be critical to reaching the quantum regime from room temperature in a variety of contemporary optomechanical systems. © 2023 Optica Publishing Group under the terms of the Optica Open Access Publishing Agreement

https://doi.org/10.1364/OPTICA.500123

1. INTRODUCTION

Room temperature quantum experiments are a longstanding pursuit of cavity optomechanics [1–3], spurred by the promise of fieldable quantum technologies [4–6] and simple platforms for fundamental physics tests [7,8]. Recently, ground state cooling has been achieved from room temperature using levitated nanoparticles [9,10]. Ponderomotive squeezing has also been achieved at room temperature, using both levitated nanoparticles [11,12] and an optically stiffened cantilever [13]. Despite this progress, however, including the recent development of ultracoherent nanomechanical resonators [14,15], room temperature quantum optomechanics with rigidly tethered nanomechanical resonators (e.g., strings and membranes) remains elusive, limited to signatures of weak optomechanical quantum correlations [2,3] and cooling to occupations of greater than 10 [16–18]. Overcoming this hurdle is important because tethered nanomechanical resonators are readily functionalized and integrated with chip-scale electronics [19], features that form the basis for optomechanical quantum technologies [4,6].

A key obstacle to room temperature quantum optomechanics is thermal intermodulation noise (TIN) [20], a form of excess optical noise produced in cavity optomechanical systems (COMSs) due to the mixing of thermomechanical noise peaks. TIN is especially pronounced in high-cooperativity tethered COMSs [16,20–23], which commonly employ nanomechanical resonators with free spectral ranges orders of magnitude smaller than the cavity linewidth [14,24]. In conjunction with the cavity's transduction nonlinearity [25], this high mode density can give rise to spectrally broadband TIN orders of magnitude in excess of shot noise [20]—a severe impediment to protocols that rely on the observability of quantum backaction, such as ground state cooling [26] and squeezing [27].

Previous reports of TIN focus on its distortion of cavity-based measurement and methods to reduce it [20]. These include reducing optomechanical coupling and cavity finesse, operating at a "magic detuning" where the leading (quadratic) transduction nonlinearity vanishes [20], multimode cooling [28], and enhancing mechanical Q. Proposals for cavity-free quantum optomechanics with ultracoherent nanomechanical resonators represent an extreme solution [29–31]. A promising compromise exploits wide-bandgap phononic crystal nanoresonators in conjunction with broadband dynamical backaction cooling [17]. Another key insight is that the phase of a resonant cavity probe is insensitive to TIN, allowing efficient feedback cooling even in the presence of nonlinear thermal noise transduction [17,20].

With this paper, we wish to highlight a complementary form of TIN—stochastic radiation pressure backaction (TINBA)—that is resilient to some of the above methods and poses an additional obstacle to room temperature quantum optomechanics. While previous studies have observed the effect of nonlinear thermal noise transduction (hereafter "thermal nonlinearity") on dynamical backaction—as an inhomogeneous broadening of the optical spring and damping effects [21]—TINBA, a type of classical intensity noise heating, is subtler, as it appears only indirectly in cavity-based measurements, and can dominate quantum backaction (QBA) even when the thermal nonlinearity is small. As a demonstration, we study TIN in a high-cooperativity, room temperature COMS based on an acoustic-frequency Si_3N_4 trampoline

coupled to a Fabry–Perot cavity (a popularly proposed system for room temperature quantum experiments [1]). Despite the thermal motion of the trampoline being 10 times smaller than the cavity linewidth, we observe TINBA as high as 20 dB in excess of thermal noise and an estimated 40 dB in excess of QBA. We show that this noise can be precisely modeled, despite its apparent complexity, and explore tradeoffs to mitigating it via its strong dependence on temperature, finesse, and detuning.

2. THEORY: QBA VERSUS TINBA

As illustrated in Fig. 1, TINBA arises due to a combination of transduction nonlinearity and radiation pressure in cavity-based readout of a multimode mechanical resonator. We here consider the observability of QBA in the presence of TINBA, focusing on a single mechanical mode with displacement coordinate x and frequency $\omega_{\rm m}$. As a figure of merit, we take the quantum cooperativity

$$C_q = \frac{S_x^{\rm QBA}}{S_x^{\rm tot} - S_x^{\rm QBA}} \approx \frac{S_x^{\rm QBA}}{S_x^{\rm th} + S_x^{\rm TIN}}, \tag{1}$$

where $S_x^{\rm QBA}[\omega]$ is the single-sided power spectral density [32] of displacement (x) produced by QBA, $S_x^{\rm tot}[\omega]$ is the total displacement spectral density—including thermal motion $S_x^{\rm th}[\omega]$ and TINBA $S_x^{\rm TIN}[\omega]$, defined below—and $S_x[\omega_{\rm m}] \equiv S_x$ denotes the spectral density on resonance.

To build a model for C_q, we first consider a single-mode COMS characterized by an optomechanical coupling:

$$\omega_{\rm c}(x) = \omega_{\rm c,0} - Gx, \tag{2}$$

where $\omega_{\rm c}$ is the cavity resonance frequency, and G (the "frequency pull parameter") characterizes the optomechanical coupling strength. In the small displacement limit, the coupled Langevin equations describing this system are [33]

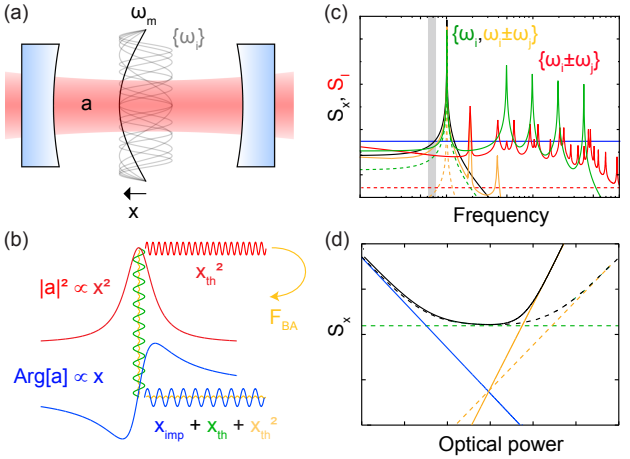

Fig. 1. (a) Multimode cavity optomechanical system (COMS) with intracavity field amplitude a and mechanical resonance frequencies ω_i. (b) Nonlinear transduction of displacement x into intensity (red) and linear transduction into phase (blue). Radiation pressure (yellow) couples intensity and phase. (c) Displacement and intensity (I) noise spectral density for resonantly probed COMS. Dashed lines: single-mode COMS with intensity dominated by shot noise (red) and total displacement (black) by thermal noise (green) and QBA (orange). Solid lines: multimode COMS with shot noise overwhelmed by TIN and QBA overwhelmed by TINBA. (d) Noise budget versus optical power for shaded region in (c).

$$m\ddot{x} + m\Gamma_{\rm m}\dot{x} + m\omega^2 x = F_{\rm th} + \hbar G|a^2|, \tag{3a}$$

$$\dot{a} = \left(i(\omega_0 - \omega_{\rm c}(x)) - \frac{\kappa}{2}\right) a + \sqrt{\kappa_{\rm in}} s_{\rm in}, \tag{3b}$$

where Eq. (3a) describes the displacement of a mechanical oscillator with mass m, resonance frequency $\omega_{\rm m}$, and damping rate $\Gamma_{\rm m}$, driven by a thermal force $F_{\rm th}$ and a radiation pressure backaction force $F_{\rm BA} = \hbar G|a^2|$; and Eq. (3b) describes the complex amplitude a of the cavity field with energy decay rate κ, driven at rate $\kappa_{\rm in}$ by an input field with amplitude $s_{\rm in}$ and frequency ω_0, and normalized so that $|a|^2 = n_{\rm c}$ is the intracavity photon number, and $|s_{\rm in}|^2$ is the input photon flux.

Linearizing Eq. (3) about small fluctuations in a yields

$$S_x[\omega] = |\chi_{\rm eff}(\omega)|^2 \left(S_F^{\rm th}[\omega] + S_F^{\rm QBA}[\omega]\right), \tag{4}$$

where $\chi_{\rm eff}(\omega) \approx (1/m)/(\omega^2 - \omega_{\rm eff}^2 - i\Gamma_{\rm eff}\omega)$ is the effective mechanical susceptibility accounting for optical stiffening $k_{\rm opt} = m\omega_{\rm eff}^2 - m\omega_{\rm m}^2$ and damping $\Gamma_{\rm opt} = \Gamma_{\rm eff} - \Gamma_{\rm m}$ [33],

$$S_F^{\rm th}[\omega] \approx 4k_B T m \Gamma_{\rm m} \tag{5}$$

is the thermal force power spectral density [34] assuming a bath temperature $T \gg \hbar\omega_{\rm m}/k_B$, and

$$S_F^{\rm QBA}[\omega] = (\hbar G n_{\rm c})^2 S_{\rm RIN}^{\rm shot}[\omega] = (\hbar G n_{\rm c})^2 \frac{8/(n_{\rm c}\kappa)}{1 + 4\left(\frac{\omega+\Delta}{\kappa}\right)^2} \tag{6}$$

is the QBA force produced by shot fluctuations of the intracavity photon number $S_{n_{\rm c}}^{\rm shot}[\omega]$ [33,35], here expressed as a relative intensity noise $S_{\rm RIN}^{\rm shot}[\omega] = S_{n_{\rm c}}^{\rm shot}[\omega]/n_{\rm c}^2$, and $\Delta = \omega_0 - \omega_{\rm c,0}$ is the laser-cavity detuning.

We hereafter specialize to the fast cavity limit $\omega_{\rm m} \ll \kappa$, in which most room temperature quantum optomechanics experiments with tethered mechanical resonators operate, including ours. In this case $C_q > 1$ requires

$$\frac{S_F^{\rm QBA}}{S_F^{\rm th}} = \frac{C_0 n_{\rm c}}{n_{\rm th}} \frac{1}{1 + 4\Delta^2/\kappa^2} > 1, \tag{7}$$

where $n_{\rm th} = \frac{k_B T}{\hbar\omega_0}$ is the thermal bath occupation, and

$$C_0 = \frac{2G^2\hbar}{m\omega_{\rm m}\Gamma_{\rm m}\kappa} = \frac{4g_0^2}{\kappa\Gamma_{\rm m}} \tag{8}$$

is the vacuum optomechanical cooperativity, expressed on the right-hand side in terms of the vacuum optomechanical coupling rate $g_0 = Gx_{\rm ZP}$, where $x_{\rm ZP} = \sqrt{\hbar/(2m\omega_{\rm m})}$ is the oscillator's zero-point motion.

Turning to TIN, we first re-emphasize that Eq. (3) considers only a single mechanical mode whose displacement is perturbatively small, $Gx \ll \kappa$. In practice, however, operating in the fast cavity limit using tethered nanomechanical resonators usually implies that many mechanical modes are simultaneously coupled to the cavity:

$$\omega_{\rm c} = \omega_{\rm c,0} - \sum_i G_i x_i. \tag{9}$$

Moreover, for a single mode designed for high cooperativity [Eq. (8)], low stiffness $m\omega_{\rm m}^2$ and high temperature can readily lead

to a root-mean-squared thermal displacement $x_{\rm th}$ exceeding the nonlinear transduction threshold

$$x_{\rm th} = \sqrt{\frac{k_B T}{m\omega_{\rm m}^2}} \gtrsim \frac{\kappa}{G} \sim \frac{\lambda}{\mathcal{F}}, \tag{10}$$

where $\mathcal{F}$ is the cavity finesse. As explored in [20], the combination of these features—multiple mechanical modes exhibiting thermal nonlinearity—can lead to broadband TIN $S_{n_c}^{\rm TIN}$ (alternatively expressed in RIN units as $S_{\rm RIN}^{\rm TIN} = S_{n_c}^{\rm TIN}/n_{\rm c}^2$) due to the mixing of thermal noise peaks. This in turn gives rise to a TINBA force:

$$S_F^{\rm TIN}[\omega] = (\hbar G n_{\rm c})^2 S_{\rm RIN}^{\rm TIN}[\omega], \tag{11}$$

which, like classical laser intensity noise [36], can drive the mechanical resonator in excess of QBA.

To analyze TINBA in the fast cavity limit, it suffices to consider the steady-state dependence of $n_{\rm c}$ on detuning, expanded to second order in deviations from the mean value Δ. For convenience, following [20], we define the relative detuning $\nu = 2\Delta/\kappa$ and its deviation $\delta\nu$, yielding

$$n_{\rm c}(\delta\nu) \propto 1 - \frac{2\nu}{1+\nu^2}\delta\nu + \frac{3\nu^2-1}{(1+\nu^2)^2}\delta\nu^2. \tag{12}$$

For a single mechanical mode, with $\delta\nu = 2Gx/\kappa$, the second term in Eq. (12) corresponds to the optical spring force $F_{\rm BA}(x) = k_{\rm opt}(\nu)x$. For a multimode optomechanical system, with $\delta\nu = \sum_n 2G_n x_n/\kappa$, the third term gives rise to intermodulation noise. To see this, using Wick's theorem [37], the spectrum of ν^2 can be expressed as the self-convolution of double-sided linear spectrum $S_{\nu\nu}[\omega]$:

$$S_{\nu^2}[\omega] = 4\int_{-\infty}^{\infty} S_{\nu\nu}[\omega']S_{\nu\nu}[\omega-\omega']\frac{d\omega'}{2\pi}, \tag{13}$$

where

$$S_{\nu\nu}[\omega] = \sum_n \frac{4G_n^2}{\kappa^2} S_{xx}^n[\omega] \tag{14}$$

is the cavity frequency noise including all mechanical modes for which $\omega_n \lesssim \kappa$. The resulting TIN

$$S_{\rm RIN}^{\rm TIN}[\omega] = \frac{(3\nu^2-1)^2}{(1+\nu^2)^4} S_{\nu^2}[\omega] \tag{15}$$

gives rise to a TINBA force [Eq. (11)]:

$$S_F^{\rm TIN}[\omega] = (\hbar G n_{\rm c})^2 \frac{(3\nu^2-1)^2}{(1+\nu^2)^4} S_{\nu^2}[\omega]. \tag{16}$$

Three features of TINBA bear emphasis. First, unlike QBA or photothermal heating (which both scale as $S_x \propto n_{\rm c}$), TINBA scales quadratically with $n_{\rm c}$. Second, unlike the optical spring, TINBA does not vanish on resonance ($\nu = 0$). In fact, it is maximal in this case, simplifying to

$$S_F^{\rm TIN}[\omega,\ \nu=0] = (\hbar G n_{\rm c})^2 S_{\nu^2}[\omega], \tag{17}$$

corresponding to $S_{\rm RIN}^{\rm TIN}[\omega] = S_{\nu^2}[\omega]$. Third, there exists a "magic" detuning $|\nu| = 1/\sqrt{3}$ at which TINBA vanishes:

$$S_F^{\rm TIN}[\omega,\ \nu = \pm 1/\sqrt{3}] = 0, \tag{18}$$

corresponding to a $\partial^2 n_{\rm c}/\partial^2\nu = 0$. However, at this detuning, the optical spring is maximized, possibly leading to instability ($k_{\rm opt} \approx -m\omega_{\rm m}^2$) for large $n_{\rm c}$.

With these features in mind, we suggest three conditions for observing QBA ($C_q \gtrsim 1$) in the presence of TIN, valid for negative detunings ($\nu < 0$) in the fast cavity limit (see Supplement 1):

$$n_{\rm c} \gtrsim (1+\nu^2)\frac{n_{\rm th}}{C_0}, \tag{19a}$$

$$Q_{\rm m} \gtrsim 2|\nu| n_{\rm th}, \tag{19b}$$

$$S_{\rm RIN}^{\rm TIN} \lesssim \frac{1}{(1+\nu^2)^2}\frac{S_\nu^{\rm ZP}}{2n_{\rm th}}, \tag{19c}$$

where $Q_{\rm m} = \omega_{\rm m}/\Gamma_{\rm m}$ is the mechanical quality factor, and $S_\nu^{\rm ZP} = (16g_0^2/\Gamma_{\rm m})/\kappa^2$ is the normalized zero-point detuning spectral density, related to the zero-point displacement spectral density $S_x^{\rm ZP} = S_x^{\rm th}/(2n_{\rm th}) = 4x_{\rm ZP}^2/\Gamma_{\rm m}$ by $S_\nu^{\rm ZP} = 4G^2 S_x^{\rm ZP}/\kappa^2$. The first two conditions are independent of TIN and correspond to $S_F^{\rm QBA} > S_F^{\rm th}$ and $k_{\rm opt} > -m\omega_{\rm m}^2$ (i.e. $\omega_{\rm eff} > 0$), respectively (see Supplement 1). The last condition implies that $S_F^{\rm TIN} \lesssim S_F^{\rm th}$ when $C_q = 1$, and is given by maximizing the relation (see Supplement 1)

$$C_q = \frac{1}{1+\nu^2}\left(\frac{S_{\rm RIN}^{\rm TIN}(G,\kappa,\nu)}{8/\kappa}n_{\rm c} + \frac{n_{\rm th}}{C_0 n_{\rm c}}\right)^{-1} \tag{20}$$

over $n_{\rm c}$, where we have emphasized the dependence of $S_{\rm RIN}^{\rm TIN}$ on system parameters and detuning.

In the next section, we explore the requirements in Eq. (19) in a popular membrane-in-the-middle platform, and show that Eq. (19c) may not be met even if Eqs. (19a) and (19b) are.

3. TRAMPOLINE-IN-THE-MIDDLE SYSTEM

Our optomechanical system consists of a Si_3N_4 trampoline resonator coupled to a Fabry–Perot cavity in the membrane-in-the-middle configuration [38]—hereafter dubbed "trampoline-in-the-middle" (TIM). As shown in Fig. 2(a), the quasi-monolithic cavity is assembled by sandwiching the Si device chip between a concave (radius 10 cm) and a plano mirror, with the trampoline positioned nearer the plano mirror to minimize diffraction loss. [This is achieved by etching the plano mirror into a mesa-like structure (see Supplement 1), as shown in Fig. 2(a).] A relatively short cavity length of $L = 415$ μm is chosen, to reduce sensitivity to laser frequency noise (see Supplement 1). The bare (without trampoline) cavity finesse is as high as $\mathcal{F} = 3\times10^4$ at wavelengths near the coating center, $\lambda = 850$ nm. To reduce thermal nonlinearity, $\mathcal{F}$ is reduced to ≈ 550 by operating at $\lambda \approx 786$ nm, yielding a cavity decay rate of $\kappa = 2\pi \times 0.65$ GHz.

Si_3N_4 trampolines are popular candidates for room temperature quantum optomechanics experiments [1,24,29], owing to their high Q-stiffness ratio. We employ an 85-nm-thick trampoline with a 200×200 μm^2 central pad, 1700×4.2 μm^2 tethers, and tether fillets designed to optimize strain-induced dissipation dilution of the fundamental mode [39], yielding $Q_m = 2.6\times10^7$ [29], $\omega_m \approx 2\pi \times 41$ kHz, and a COMSOL-simulated effective mass of $m = 12$ ng. Care was taken to mount the trampoline without introducing loss; nevertheless, two small dabs of adhesive reduced $Q_{\rm m}$ to 7.8×10^6 (we speculate that this is due to

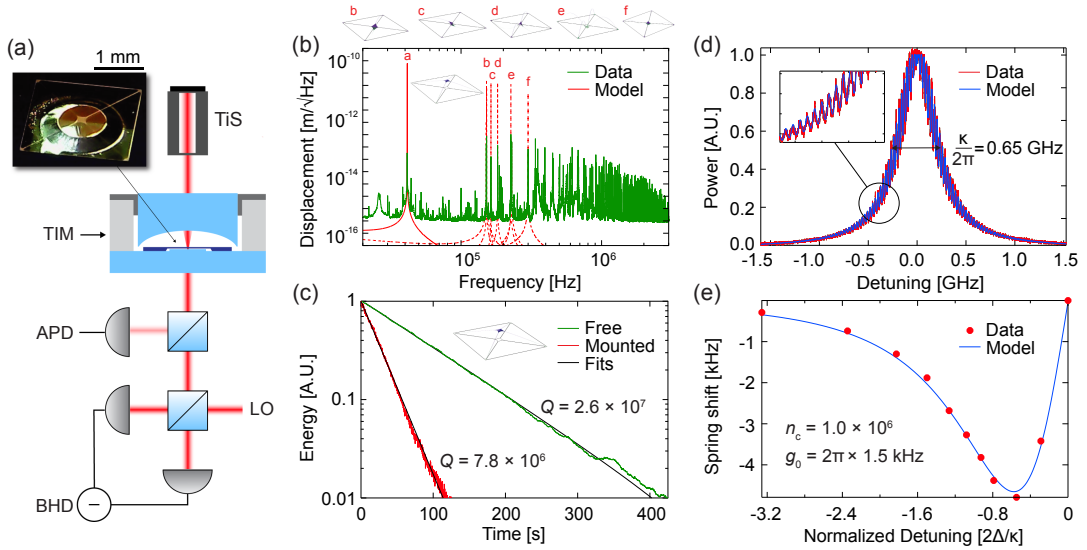

Fig. 2. Trampoline-in-the-middle (TIM) cavity optomechanical system. (a) Experimental setup: the TIM cavity is driven by a titanium sapphire laser (TiS) and probed in transmission with an avalanche photodiode (APD) and balanced homodyne detector (BHD). The BHD local oscillator (LO) is derived from the same TiS. (b) Displacement measurement using a resonant probe and the BHD tuned to the phase quadrature. Thermal noise models for the first five trampoline modes (a)–(d) are overlayed. (c) Ringdown measurements of the fundamental trampoline before (green) and after (red) mounting inside the TIM cavity. (d) Detuning sweep over cavity resonance, fit with a model that includes the thermal motion of the trampoline fundamental mode. (e) Measurement of the optical spring shift versus detuning, used to determine the intracavity photon number.

hybridization with low-Q chip modes [40], as evidenced by the satellite noise peaks in Fig. 4.) The resulting thermal force noise $S_F^{\rm th} \approx 8 \times 10^{-17}\ \mathrm{N}/\sqrt{\mathrm{Hz}}$ is in principle sufficient to observe QBA ($C_q \sim 1$) with an input power of $\sim$10 mW at $\mathcal{F} \sim 10^3$. Challenging this prospect is the fact that the trampoline's thermal motion, $x_{\rm th} = 0.07$ nm, is near the nonlinear transduction threshold [Eq. (10)] at $\mathcal{F} \sim 10^3$. Moreover, $\kappa/\omega_{\rm m} \sim 10^4$ allows many higher-order trampoline modes to be coupled to the cavity field [Fig. 2(b)], satisfying the conditions for strong TIN.

Measurements characterizing the nonlinearity and cooperativity of our TIM system are shown in Figs. 2(d) and 2(e). A hallmark of thermal nonlinearity is modulation of the steady-state cavity response, as shown in Fig. 2(d). Here the cavity length is swept across resonance with strong optomechanical coupling, corresponding to the trampoline positioned between a node and an antinode of the intracavity standing wave [41]. Fitting the transmitted power to $P_{\rm out}(\nu(t)) \propto 1/(1 + (\nu + 8Gx_{\rm th}\cos(\omega_{\rm m}\nu/\dot{\nu})/\kappa))^2)$ (where $\dot{\nu}$ is the constant slew rate of the detuning sweep) yields $Gx_{\rm th}/\kappa \approx 0.04$ (see Supplement 1), corresponding to $g_0 = Gx_{\rm th}/\sqrt{2n_{\rm th}} \sim 2\pi \times 1$ kHz. A more careful estimate of $g_0 = 2\pi \times 1.5$ kHz was obtained using the frequency sideband calibration method [42], suggesting a vacuum cooperativity of $C_0 \approx 3$. In the experiment below, for each input power $P_{\rm in}$, the intracavity photon number $n_{\rm c}$ is determined by recording the optical spring shift versus detuning and comparing to a model, $\Delta\omega_{\rm opt} \approx k_{\rm opt}/(2m\omega_{\rm m}) \approx \Gamma_{\rm m} C_0 n_{\rm c}(\nu = 0)\nu/(1 + \nu^2)^2$ [Fig. 2(e)]. For all measurements, the thermal nonlinearity is reduced by measurement-based feedback cooling of the fundamental mode. Full details and methods are presented in Supplement 1.

4. OBSERVATION OF TIN BACKACTION

We now explore TIN in our TIM system and present evidence that TINBA overwhelms QBA at a sufficiently high intracavity photon number. To this end, the cavity is probed on resonance ($\nu = 0$) with a titanium-sapphire laser (M-Squared Solstis) pre-stabilized with a broadband electro-optic intensity noise eater (see Supplement 1). The output field $s_{\rm out} \propto \sqrt{\kappa}a$ is monitored with two detectors. A balanced homodyne detector records the phase of $s_{\rm out}$, which encodes the trampoline displacement, $\mathrm{Arg}[s_{\rm out}] \propto x$, with a shot-noise-limited imprecision of $S_x^{\rm imp} \geq S_x^{\rm ZP}/(8C_0 n_{\rm c})$. An avalanche photodiode (APD) records the output intensity $|s_{\rm out}|^2 \propto n_{\rm c}$ and is also used to lock the cavity using the Pound–Drever–Hall technique (see Supplement 1).

TIN couples directly to intracavity intensity and indirectly to mechanical displacement, via TINBA. We explore this in Fig. 3, by comparing the intensity and phase fluctuations of an optical field passed resonantly through the TIM cavity. An input power of $P_{\rm in} = 0.2$ mW is used, corresponding to $n_{\rm c} = 4\eta P_{\rm in}/(\hbar\omega_{\rm c}\kappa) = 4 \times 10^5$ intracavity photons (with $\eta = 0.4$ determined from the optical spring shift) and an ideal quantum cooperativity of $C_q = 7 \times 10^{-3}$(in principle large enough to observe optomechanical quantum correlations [2,3]). The phase noise spectrum is calibrated in displacement units by bootstrapping to a model for the fundamental thermomechanical noise peak (see Supplement 1), yielding the apparent displacement noise spectrum

$$S_y[\omega] \equiv S_x[\omega] + S_x^{\rm imp}[\omega]. \tag{21}$$

As seen in Fig. 3(a), $S_y[\omega]$ is dominated by thermal noise near mechanical resonances and shot noise far from resonance. The intensity noise [Fig. 3(b)] meanwhile exceeds shot noise and features numerous peaks at intermediate frequencies, suggestive of TIN. To confirm this hypothesis, in Fig. 3(b), we overlay the measured intensity noise with our TIN model [Eq. (13)] using the phase-noise-inferred thermomechanical noise $S_y[\omega] - S_x^{\rm imp}[\omega] \approx S_x^{\rm th}[\omega]$ as an input. We observe strong

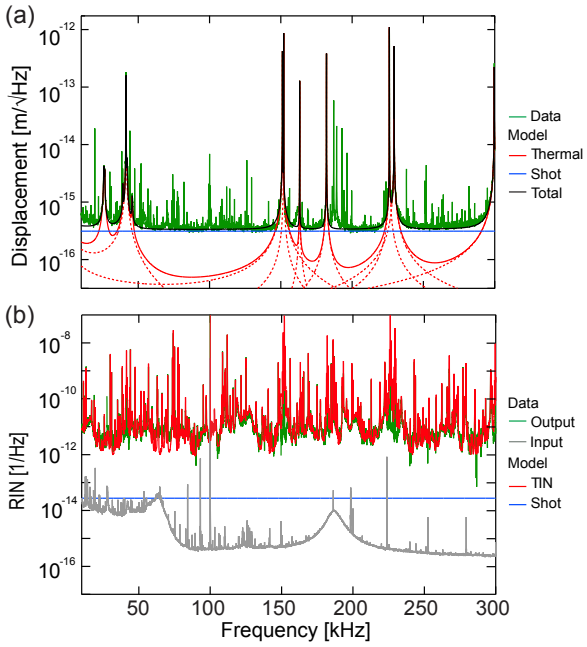

Fig. 3. Thermal intermodulation noise (TIN) in TIM system. (a) Low-frequency part of the phase measurement in Fig. 2(b) (green), compared to models of the thermal motion of the first seven trampoline modes (dotted red), their incoherent sum (solid red), shot noise (blue), and total noise (black). (b) Simultaneously recorded intensity noise (green), normalized by the mean intensity (RIN). Red curve is a TIN model (see main text), blue is a shot noise model, and gray is the measurement of the input laser RIN, after the noise eater (see Supplement 1).

agreement over the full measurement band, as highlighted in Fig. 3(b).

We now turn our attention to the spurious peaks in the phase noise spectrum in Fig. 3(a), which we argue is displacement produced by TINBA. To this end, in Fig. 4, we compare $S_y[\omega]$ at different probe powers, focusing on Fourier frequencies near the fundamental trampoline resonance. Qualitatively, as shown in Figs. 4(a) and 4(b), we observe an increase in the apparent displacement at larger powers, with a shape that is consistent with the measured intensity noise multiplied by the mechanical susceptibility. To confirm that this is TINBA, in Fig. 4(d) we plot $S_y[\omega_m + \delta]$ at an offset $\delta \gg \Gamma_m$ versus input power in the range $P_{in} \in [10\,\mu W, 1.1\,mW]$ ($n_c \in [1.7 \times 10^4, 2.2 \times 10^6]$). The observed quadratic scaling with P_{in} is consistent with TINBA and distinct from QBA and photoabsorption heating. The absolute magnitude of the displacement moreover agrees quantitatively well with our TINBA model, $S_x[\omega_m + \delta] \approx S_{RIN}[\omega_m + \delta]/(m\omega_m^2\Gamma_m^2)^2$ (black line), allowing for statistical uncertainty (gray shading) due to fluctuations in the measured $S_{RIN}[\omega]$.

As an additional consistency check, we measure the coherence between the phase and intensity noise, allowing us to rule out artifacts such as imperfect cancellation of intensity noise in the balanced homodyne receiver. We define the coherence between signals a and b as $C_{ab}[\omega] = |S_{ab}[\omega]|^2/(S_a[\omega]S_b[\omega])$ [43], where $S_{ab}[\omega]$ is the cross-spectrum of a and b, so that $C_{ab}[\omega] = 1$ for perfectly correlated or anti-correlated signals, and Arg$[S_{ab}]$ characterizes the relative phase of the correlated signal components. Figure 4(c) shows the coherence of the phase and intensity noise measurements with $n_c = 2 \times 10^6$, together with a model that predicts the coherence based on the measured TIN noise and the mechanical susceptibility. A high degree of coherence is observed over a ∼100 kHz bandwidth surrounding the fundamental

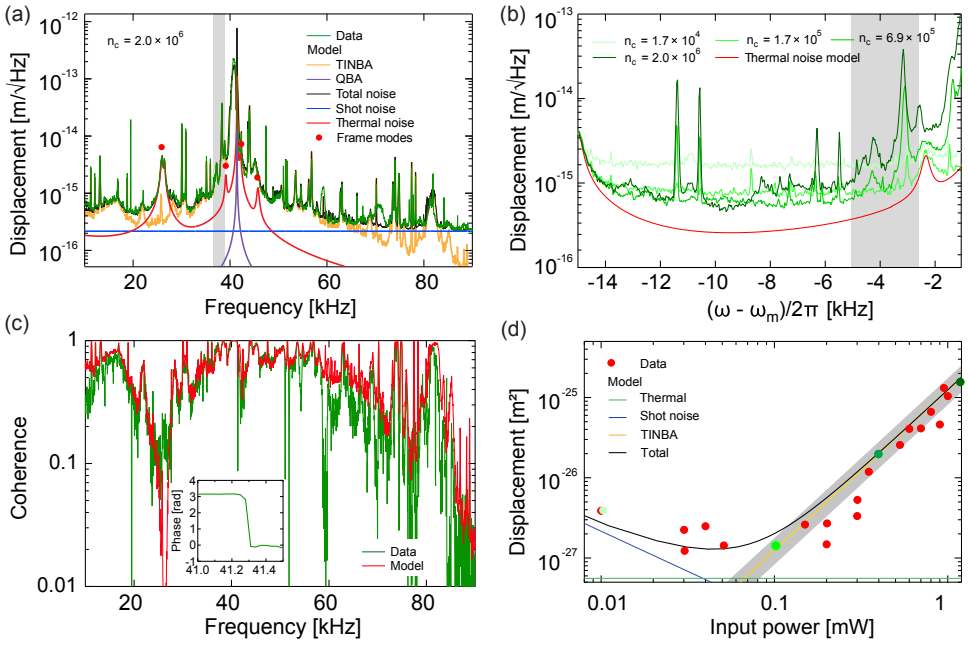

Fig. 4. Evidence for TINBA in a strong displacement measurement. (a) Displacement noise near the fundamental trampoline resonance ω_m, with models for various components overlaid and shading for integration region in (d). (b) Noise spectra at different powers versus offset frequency $\omega - \omega_m$. Shot noise dominates at low power and large offset frequencies, scaling inversely with power. At smaller offset frequencies, noise gradually increases with power, due to TINBA. (c) Coherence between the noise in (a) and a simultaneously recorded intensity noise. Values near unity imply a high degree of correlation. Inset: phase of the coherence function. The π phase change on resonance is due the mechanical susceptibility. (d) Noise integrated over the frequency range shaded in (a), overlaid with models for shot noise (blue), thermal noise (green), and TINBA (yellow). Gray shading is the uncertainty of the TINBA model due to statistical variation of the measured TIN. Points from (b) are denoted with their respective color.

resonance. Moreover, near resonance, the argument of the coherence undergoes a π-phase shift, indicative of the response of the mechanical susceptibility, and consistent with TINBA-driven motion. Full details about models and measurements can be found in Supplement 1.

5. IMPLICATIONS FOR QUANTUM OPTOMECHANICS EXPERIMENTS

TIN backaction currently limits the quantum cooperativity of our TIM system. For example, at the highest intracavity photon number in Fig. 4, $n_c = 2\times10^6$, $S_x^{\rm TIN}/S_x^{\rm th}\approx 10^2$, and $S_x^{\rm TIN}/S_x^{\rm QBA} = (S_x^{\rm TIN}/S_x^{\rm th})/C_q^0 \approx 2500$, implying that $C_q \approx 4\times10^{-4}$ instead of the ideal value, $C_q^0 = C_0 n_c/n_{\rm th} = 0.04$. As implied by Eq. (19c), this could have been anticipated by comparing the measured TIN to the *a priori* zero-point frequency noise $S_v^{\rm ZP} = 4C_0/\kappa \approx 3\times10^{-9}$ scaled by the thermal occupation $n_{\rm th}\approx 1.5\times10^8$. In our case, $S_{\rm RIN}^{\rm TIN}\approx 10^{-11}{\rm Hz}^{-1}$, yielding $C_q \lesssim 10^{-3}$ according to Eq. (20):

$$C_q(\nu=0) = \left(\frac{S_{\rm TIN}^{\rm RIN}}{8/\kappa}n_c + \frac{n_{\rm th}}{C_0 n_c}\right)^{-1} \le \sqrt{\frac{S_v^{\rm ZP}/2n_{\rm th}}{S_{\rm TIN}^{\rm RIN}}}. \quad (22)$$

The lower bound of Eq. (22) [and more generally, Eq. (20)] applies to any form of classical intensity noise, and results from the fact that classical intensity noise increases quadratically with n_c, while shot noise increases linearly with n_c. There is, therefore, always a probe strength at which classical backaction overwhelms QBA. To increase this threshold, one must either increase the zero-point spectral density or reduce the intensity noise, leveraging, if possible, the different scaling of these noise terms with system parameters.

In the case of TINBA, which originates from thermal nonlinearity [Eq. (10)], inroads can be made by leveraging the dependence of the nonlinearity on G, κ, and ν. For example, the fact that $S_F^{\rm TIN}\propto(G/\kappa)^4$ and $S_F^{\rm QBA}\propto(G/\kappa)^2$ suggests that TINBA can be mitigated by using a higher κ (lower-finesse $\mathcal{F}$) cavity. In Fig. 5(b) we consider this strategy for our TIM system using the above experimental parameters and $\nu=0$. Evidently, $C_q\sim1$ is possible with 100-fold lower $\mathcal{F}$; however, it would require a proportionately larger laser power. This is problematic because of photothermal heating and increased demands on classical laser intensity noise suppression. Figures 5(a) and 5(b) show the same computation at $T=4$ K, revealing that power demands are relaxed in proportion to T, since $S_F^{\rm TIN}\propto T^2$. This observation reaffirms the demands of room temperature quantum optomechanics and, conversely, the advantages of cryogenic pre-cooling.

Finally, we re-emphasize the strong detuning dependence of TIN and TINBA. Operating at the magic-detuning $\nu=1/\sqrt{3}$, as shown in Fig. 5(c), can eliminate TIN in the optical intensity; however, as evident in the blue data, the phase response of the cavity becomes nonlinear, potentially preventing the observation of quantum correlations generated via the optomechanical interaction. Moreover, in the regime of strong QBA, the associated optical spring (maximal at $\nu=1/\sqrt{3}$ in the fast cavity limit) can be substantial. To avoid instability ($\omega_{\rm eff}=0$), one strategy is to use a dual-wavelength probe with $\nu=\pm1/\sqrt{3}$, but this does not resolve the phase nonlinearity issue. Another promising strategy—not considered in our theoretical analysis—is to exploit optical damping at $\nu\neq0$ to realize multimode cooling [17]. The success of this strategy will depend on the details of the system and may benefit by operating in an intermediate regime between the fast and slow cavity limits.

6. CONCLUSION

We have explored the effect of thermal intermodulation noise (TIN) on the observability of radiation pressure quantum backaction (QBA) in a room temperature cavity optomechanical system and argued that TIN backaction (TINBA) can overwhelm QBA under realistic conditions. As an illustration, we studied the effects of TINBA in a high-cooperativity trampoline-in-the-middle cavity optomechanical system and found that it overwhelmed thermal noise and QBA by several orders of magnitude. The conditions embodied by our TIM system—transduction nonlinearity, large thermal motion, and a multimode mechanical resonator—can be found in a wide variety of room temperature quantum optomechanics experiments based on tethered nanomechanical resonators, including an emerging class of systems based on ultracoherent phononic crystal nanomembranes and strings [16,17]. Anticipating and mitigating TINBA in these systems may therefore be a key step to operating them in the quantum regime. In addition to increasing Q, a program combining multimode coherent [17] or measurement-based [28] feedback cooling, dual-probes at the "magic detuning" [44], and/or engineering of the effective mass and frequency spectrum [45] may be advantageous.

Funding. National Science Foundation (ECCS-1725571, ECCS-1945832).

Acknowledgment. The authors thank Charles Condos for assistance in refining the experimental apparatus and Ute Drechsler for fabricating the mesa mirrors. CMP acknowledges support from the ARCS Foundation, an Amherst

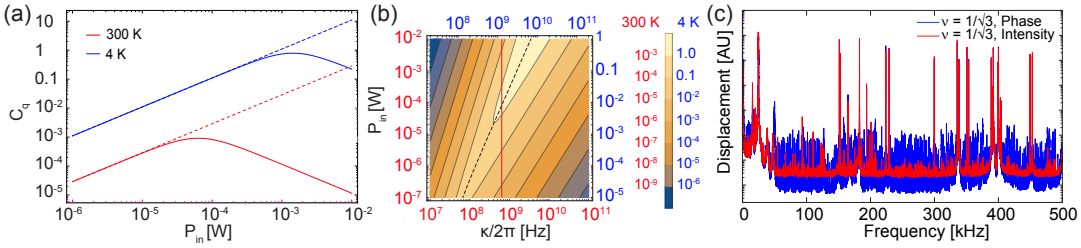

Fig. 5. Strategies for mitigating TINBA. (a) Estimated quantum cooperativity C_q of TIM system at $T=300$ K (red) and 4 K (blue) assuming no TIN (dashed line) and parameters in the experiment (solid line, $S_{\rm RIN}^{\rm TIN}\approx10^{-11}$ Hz^{-1}, $g_0=2\pi\times1.5$ kHz, and $\kappa=2\pi\times650$ MHz). Cryogenic operation reduces thermal noise and TIN, increasing the maximum C_q by $1/T^2$. (b) C_q of TIM system as a function of linewidth and input power, for $T=300$ K and 4 K. The red line indicates the slice shown in (a). The dashed line indicates the maximum C_q for a given κ and $P_{\rm in}$. (c) Readout of the TIM cavity at the "magic detuning," showcasing a decrease in TIN in the intensity noise (red), but an increase of TIN in the phase (displacement) noise (blue).

College Fellowship, and a Grant in Aid of Research from Sigma Xi. ARA acknowledges support from a CNRS-UArizona iGlobes fellowship. The reactive ion etcher used for this study was funded by NSF.

Disclosures. The authors declare no conflicts of interest.

Data availability. Data underlying the results presented in this paper are not publicly available at this time but may be obtained from the authors upon reasonable request.

Supplemental document. See Supplement 1 for supporting content.

REFERENCES AND NOTES

1. R. Norte, J. Moura, and S. Gröblacher, "Mechanical resonators for quantum optomechanics experiments at room temperature," Phys. Rev. Lett. **116**, 147202 (2016).
2. T. P. Purdy, K. E. Grutter, K. Srinivasan, and J. M. Taylor, "Quantum correlations from a room-temperature optomechanical cavity," Science **356**, 1265–1268 (2017).
3. V. Sudhir, R. Schilling, S. Fedorov, H. Schütz, D. Wilson, and T. Kippenberg, "Quantum correlations of light from a room-temperature mechanical oscillator," Phys. Rev. X **7**, 031055 (2017).
4. M. Metcalfe, "Applications of cavity optomechanics," Appl. Phys. Rev. **1**, 031105 (2014).
5. M. Rademacher, J. Millen, and Y. L. Li, "Quantum sensing with nanoparticles for gravimetry: when bigger is better," Adv. Opt. Technol. **9**, 227–239 (2020).
6. S. Barzanjeh, A. Xuereb, S. Gráblacher, M. Paternostro, C. A. Regal, and E. M. Weig, "Optomechanics for quantum technologies," Nat. Phys. **18**, 15–24 (2022).
7. G. Gasbarri, A. Belenchia, M. Carlesso, S. Donadi, A. Bassi, R. Kaltenbaek, M. Paternostro, and H. Ulbricht, "Testing the foundation of quantum physics in space via interferometric and non-interferometric experiments with mesoscopic nanoparticles," Commun. Phys. **4**, 155 (2021).
8. D. Carney, G. Krnjaic, D. C. Moore, C. A. Regal, G. Afek, S. Bhave, B. Brubaker, T. Corbitt, J. Cripe, N. Crisosto, and A. Geraci, "Mechanical quantum sensing in the search for dark matter," Quantum Sci. Technol. **6**, 024002 (2021).
9. U. Delić, M. Reisenbauer, K. Dare, D. Grass, V. Vuletić, N. Kiesel, and M. Aspelmeyer, "Cooling of a levitated nanoparticle to the motional quantum ground state," Science **367**, 892–895 (2020).
10. L. Magrini, P. Rosenzweig, C. Bach, A. Deutschmann-Olek, S. G. Hofer, S. Hong, N. Kiesel, A. Kugi, and M. Aspelmeyer, "Real-time optimal quantum control of mechanical motion at room temperature," Nature **595**, 373–377 (2021).
11. L. Magrini, V. A. Camarena-Chávez, C. Bach, A. Johnson, and M. Aspelmeyer, "Squeezed light from a levitated nanoparticle at room temperature," Phys. Rev. Lett. **129**, 053601 (2022).
12. A. Militaru, M. Rossi, F. Tebbenjohanns, O. Romero-Isart, M. Frimmer, and L. Novotny, "Ponderomotive squeezing of light by a levitated nanoparticle in free space," Phys. Rev. Lett. **129**, 053602 (2022).
13. N. Aggarwal, T. J. Cullen, J. Cripe, G. D. Cole, R. Lanza, A. Libson, D. Follman, P. Heu, T. Corbitt, and N. Mavalvala, "Room-temperature optomechanical squeezing," Nat. Phys. **16**, 784–788 (2020).
14. Y. Tsaturyan, A. Barg, E. S. Polzik, and A. Schliesser, "Ultracoherent nanomechanical resonators via soft clamping and dissipation dilution," Nat. Nanotechnol. **12**, 776–783 (2017).
15. A. H. Ghadimi, S. A. Fedorov, N. J. Engelsen, M. J. Bereyhi, R. Schilling, D. J. Wilson, and T. J. Kippenberg, "Elastic strain engineering for ultralow mechanical dissipation," Science **360**, 764–768 (2018).
16. J. Guo, R. Norte, and S. Gröblacher, "Feedback cooling of a room temperature mechanical oscillator close to its motional ground state," Phys. Rev. Lett. **123**, 223602 (2019).
17. S. A. Saarinen, N. Kralj, E. C. Langman, Y. Tsaturyan, and A. Schliesser, "Laser cooling a membrane-in-the-middle system close to the quantum ground state from room temperature," Optica **10**, 364–372 (2023).
18. P. Vezio, M. Bonaldi, A. Borrielli, F. Marino, B. Morana, P. Sarro, E. Serra, and F. Marin, "Optical self-cooling of a membrane oscillator in a cavity optomechanical experiment at room temperature," arXiv, arXiv:2305.14903 (2023).
19. K. Ekinci and M. Roukes, "Nanoelectromechanical systems," Rev. Sci. Instrum. **76**, 061101 (2005).
20. S. A. Fedorov, A. Beccari, A. Arabmoheghi, D. J. Wilson, N. J. Engelsen, and T. J. Kippenberg, "Thermal intermodulation noise in cavity-based measurements," Optica **7**, 1609–1616 (2020).
21. R. Leijssen, G. R. La Gala, L. Freisem, J. T. Muhonen, and E. Verhagen, "Nonlinear cavity optomechanics with nanomechanical thermal fluctuations," Nat. Commun. **8**, 16024 (2017).
22. J.-B. Béguin, Z. Qin, X. Luan, and H. Kimble, "Coupling of light and mechanics in a photonic crystal waveguide," Proc. Natl. Acad. Sci. USA **117**, 29422–29430 (2020).
23. G. Brawley, M. Vanner, P. E. Larsen, S. Schmid, A. Boisen, and W. Bowen, "Nonlinear optomechanical measurement of mechanical motion," Nat. Commun. **7**, 10988 (2016).
24. C. Reinhardt, T. Müller, A. Bourassa, and J. C. Sankey, "Ultralow-noise SiN trampoline resonators for sensing and optomechanics," Phys. Rev. X **6**, 021001 (2016).
25. C. Doolin, B. D. Hauer, P. H. Kim, A. J. R. MacDonald, H. Ramp, and J. P. Davis, "Nonlinear optomechanics in the stationary regime," Phys. Rev. A **89**, 053838 (2014).
26. D. J. Wilson, V. Sudhir, N. Piro, R. Schilling, A. Ghadimi, and T. J. Kippenberg, "Measurement-based control of a mechanical oscillator at its thermal decoherence rate," Nature **524**, 325–329 (2015).
27. T. P. Purdy, P.-L. Yu, R. W. Peterson, N. S. Kampel, and C. A. Regal, "Strong optomechanical squeezing of light," Phys. Rev. X **3**, 031012 (2013).
28. C. Sommer, A. Ghosh, and C. Genes, "Multimode cold-damping optomechanics with delayed feedback," Phys. Rev. Res. **2**, 033299 (2020).
29. C. M. Pluchar, A. R. Agrawal, E. Schenk, D. J. Wilson, and D. J. Wilson, "Towards cavity-free ground-state cooling of an acoustic-frequency silicon nitride membrane," Appl. Opt. **59**, G107–G111 (2020).
30. J. R. Pratt, A. R. Agrawal, C. A. Condos, C. M. Pluchar, S. Schlamminger, and D. J. Wilson, "Nanoscale torsional dissipation dilution for quantum experiments and precision measurement," Phys. Rev. X **13**, 011018 (2023).
31. S. Hao, R. Singh, J. Zhang, and T. P. Purdy, "Cavity-less quantum optomechanics with nanostring mechanical resonators," in *Frontiers in Optics/Laser Science* (OSA, 2020), paper FW5C.4.
32. In the main text, $S_x[\omega]$ represents the single-sided power spectral density of x, and $S_{xx}[\omega]$ represents the double-sided power spectral density. These quantities are related by $S_x[\omega] = 2S_{xx}[\omega > 0]$, and normalized such that $\langle x^2 \rangle = \int_0^\infty S_x[\omega] \mathrm{d}\omega/(2\pi)$.
33. M. Aspelmeyer, T. J. Kippenberg, and F. Marquardt, "Cavity optomechanics," Rev. Mod. Phys. **86**, 1391–1452 (2014).
34. P. R. Saulson, "Thermal noise in mechanical experiments," Phys. Rev. D **42**, 2437–2445 (1990).
35. F. Marquardt, J. P. Chen, A. A. Clerk, and S. Girvin, "Quantum theory of cavity-assisted sideband cooling of mechanical motion," Phys. Rev. Lett. **99**, 093902 (2007).
36. P. Verlot, A. Tavernarakis, C. Molinelli, A. Kuhn, T. Antoni, S. Gras, T. Briant, P.-F. Cohadon, A. Heidmann, L. Pinard, C. Michel, R. Flaminio, M. Bahriz, O. Le Traon, I. Abram, A. Beveratos, R. Braive, I. Sagnes, and I. Robert-Philip, "Towards the experimental demonstration of quantum radiation pressure noise," C. R. Physique **12**, 826–836 (2011).
37. L. Isserlis, "On a formula for the product-moment coefficient of any order of a normal frequency distribution in any number of variables," Biometrika **12**, 134–139 (1918).
38. J. D. Thompson, B. M. Zwickl, A. M. Jayich, F. Marquardt, S. M. Girvin, and J. G. E. Harris, "Strong dispersive coupling of a high-finesse cavity to a micromechanical membrane," Nature **452**, 72–75 (2008).
39. P. Sadeghi, M. Tanzer, S. L. Christensen, and S. Schmid, "Influence of clamp-widening on the quality factor of nanomechanical silicon nitride resonators," J. Appl. Phys. **126**, 165108 (2019).
40. M. H. de Jong, M. A. ten Wolde, A. Cupertino, S. Gröblacher, P. G. Steeneken, and R. A. Norte, "Mechanical dissipation by substrate–mode coupling in sin resonators," Appl. Phys. Lett. **121**, 032201 (2022).
41. A. M. Jayich, J. C. Sankey, B. M. Zwickl, C. Yang, J. D. Thompson, S. M. Girvin, A. A. Clerk, F. Marquardt, and J. G. E. Harris, "Dispersive optomechanics: a membrane inside a cavity," New J. Phys. **10**, 095008 (2008).
42. M. L. Gorodetksy, A. Schliesser, G. Anetsberger, S. Deleglise, and T. J. Kippenberg, "Determination of the vacuum optomechanical coupling rate using frequency noise calibration," Opt. Express **18**, 23236–23246 (2010).

43. T. P. Purdy, R. W. Peterson, and C. A. Regal, "Observation of radiation pressure shot noise on a macroscopic object," Science **339**, 801–804 (2013).
44. T. Corbitt, Y. Chen, E. Innerhofer, H. Müller-Ebhardt, D. Ottaway, H. Rehbein, D. Sigg, S. Whitcomb, C. Wipf, and N. Mavalvala, "An all-optical trap for a gram-scale mirror," Phys. Rev. Lett. **98**, 150802 (2007).
45. G. L. Gala, J. P. Mathew, P. Neveu, and E. Verhagen, "Nanomechanical design strategy for single-mode optomechanical measurement," J. Phys. D **55**, 225101 (2022).

98.191.187.197 (b 2024-01-01 11:52:15)